

Modelling and Analysis of the Dynamic Behavior of a Double Cylinder Inline 650cc Gasoline Engine with Crank Angle 0o for Rubber Mount

Harus Laksana Guntur¹ and Karina Yulia¹

Abstract—This paper presents a numerical study and analysis of the dynamic behavior of a double cylinder inline 650cc gasoline engine with crank angle 0o for rubber mount. Numerical study was done by mathematically modeling a double cylinder inline 650cc gasoline engine with crank angle 0o for rubber mount and simulating its dynamic behavior for 3 different connecting rod lengths:115.6mm, 125.6mm, and 135.6mm. Its mathematical model was developed from the physical model of engine produced by local manufacturer. All parameters used in the simulation are based on the engine specification provided by the manufacturer. In the mathematical model, connecting rod length was varied to investigate its influence to the engine's dynamic behavior. Here, the engine system was modeled as a spring-mass-damper system excited by a periodic force produced by the cylinder working pressure with various excitation frequencies from 1000rpm to 5000rpm. The engine's dynamic behavior was indicated by vertical motion (bouncing) and angular motion (pitching) of the engine mass, which is presented in displacement, velocity and acceleration. The results show that connecting rod length does not influence the engine's dynamic behavior. Further, the increase in engine's angular speed/excitation frequency influence significantly the engine's dynamic behavior. The detail results of this study are reported and discussed in the paper.

Keywords—Double Cylinder Engine, Crank Angle, Dynamic Behavior, Rubber Mount, Vibration Response of Engine.

I. INTRODUCTION

In developing engine, the dynamic behavior/vibration of an engine due to its cylinder pressure is very important to analyze. The change in the crank angle and connecting rod length will yield different dynamic characteristics of engine. Two type of engine mounts are widely used in the automotive industry to isolate the vibration, i.e. hydraulic mount and rubber mount. Hydraulic mount has been used in the automotive industry since the mid-1980s to provide an adaptive vibration isolation system for the engine sturcture to meet increasing customer demand for quieter and smoother riding vehicles [1][2]. The hydraulic mount was introduced to provide a dual damping mode passive vibration isolator to control high-amplitude, low-frequency road-induced vibrations and low-amplitude, high-frequency engine-induced vibrations [3][4].

Prior to the development of an engine, numerical study on the dynamic behavior is very important to be done. Colgate et al reported in his paper the result of his work on modeling of a hydraulic engine mount focusing on response to sinusoidal and composition [5]. Adiguna et al carried out a numerical study to investigate the transient response of a hydraulic engine mount [6]. Meanwhile, very few papers report the study on the dynamic behaviour of an engine with ruber mount. When low cost and simplicity are the main purpose in producing the vehicle, ruber mount is the best choise instead of hydraulic mount.

In this research a numerical study and analysis of the dynamic behavior of a double cylinder inline 650cc

gasoline engine with crank angle 0o for rubber mount was done. In the mathematical model, connecting rod length was varied to investigate its influence to the engine's dynamic behavior. Here, the engine system was modeled as a spring-mass-damper system excited by a periodic force produced by the cylinder working pressure with various excitation frequencies from 1000rpm to 5000rpm. The engine's dynamic behavior was indicated by vertical motion (bouncing) and angular motion (pitching) of the engine mass, which is presented in displacement, velocity and acceleration. The detail results of this study are reported and discussed in the paper.

II. PROBLEM FORMULATION

A. Physical Model and Properties of the Engine

Figure 1 shows the physical model of the double cylinder inline 650cc gasoline engine with crank angle 0o used as the object for the numerical study. The engine properties are shown in Table 1. Several properties, such as: center mass and inertia of all components, are obtained by redrawing the engine parts using drawing software, as shown in figure 2.

B. Excitation Force by the Cylinder Pressure

Figure 3 shows the cycle of cylinder pressure for one cylinder in a double cylinder inline 650cc gasoline engine with crank angle 0° obtained from measurement result. The engine is four strokes engine and has 720° for one full cycle, and the phase lag between cylinder 1 and 2 is 360°. By assuming that all dynamic components of the engine are balance, the cylinder pressure will become the main source of vibration to the engine. Figure 4 shows the cylinder pressure for cyinder 1 and 2 with phase lag of 360°. From the cylinder pressure, the excitation force is obtained by mulitplying the cyinder pressure by the piston frontal area.

¹Harus Laksana Guntur and Karina Yulia are with Departement of Mechanical Engineering, Faculty of Industrial Technology, Institut Teknologi Sepuluh Nopember, Surabaya, 60111, Indonesia. E-mail: haruslg@me.its.ac.id.

The excitation force from the cylinder pressure will be transmitted to the engine through the connecting rod and crank shaft. Figure 5 shows the kinematic diagram of the cylinder, connecting rod and crank shaft. Based on the kinematic diagram, the angular acceleration of the connecting rod is defined by Eq.(1).

$$\alpha_d = \frac{L_s(\alpha_s \cos \theta - \omega_s^2 \sin \theta)}{L_d \sqrt{1 - \frac{L_s^2 \sin^2 \theta}{L_d^2}}} + \frac{\omega_s^2 L_s^3 \cos^2 \theta \sin \theta}{L_d^2 \sqrt{1 - \frac{L_s^2 \sin^2 \theta}{L_d^2}}} \quad (1)$$

The acceleration of the connecting rod's center of mass for the y and x direction can be obtained by Eq.(2) and (3), respectively.

$$a_{ry} = -L_s \alpha_s \sin \theta - L_s \omega_s^2 \cos \theta - \frac{\alpha_s L_g L_s^2 \sin 2\theta}{2L_d^2 \sqrt{1 - \frac{L_s^2 \sin^2 \theta}{L_d^2}}} - \frac{1}{L_d^2 \left(2 - \frac{2L_s^2 \sin^2 \theta}{L_d^2} \right)} \left(\omega_s^2 L_g L_s^2 \left[2 \cos 2\theta \sqrt{1 - \frac{L_s^2 \sin^2 \theta}{L_d^2}} + \frac{L_s^2 \sin^2 2\theta}{2L_d^2 \sqrt{1 - \frac{L_s^2 \sin^2 \theta}{L_d^2}}} \right] \right) \quad (2)$$

$$a_{rx} = L_s \alpha_s \cos \theta - L_s \omega_s^2 \sin \theta - \frac{L_g L_s \alpha_s \cos \theta}{L_d} + \frac{L_g L_s \omega_s \sin \theta}{L_d} \quad (3)$$

The force of the crank pin in the y and x direction can be obtained by Eq.(4) and (5), respectively.

$$F_{ay} = M_d a_{ry} + F \quad (4)$$

$$F_{ax} = \frac{1}{L_d} \left(\frac{I_{xx} \alpha_d - F_{ay} L_g - F(L_d - L_g) \sin \beta}{\cos \beta} + M_d a_{rx} (L_d - L_g) \right) \quad (5)$$

Therefore, the excitation force applied on engine body can be determined by Eq.(6).

$$F_y = F_{ay} \cos \theta + F_{ax} \sin \theta \quad (6)$$

C. Mathematical Model of the Engine Dynamics

Based on the physical model of the engine, the mathematical model of the engine dynamic, which consist of mass, stiffness and damper can be developed. Figure 6 and 7 show the mathematical model of double cylinder inline 650cc gasoline engine with crank angle 0° for front view and side view, respectively. The excitation force from the cylinder pressure $F_1(t)$ and $F_2(t)$ transmitted into the engine body are defined by Eq.(6). From the free body force diagram shown in figure 8, the equilibrium of force yields the following equations:

$$\sum F = 0 \quad (7)$$

$$M_e \ddot{y} + K_{ml} \cdot y + C_{ml} \cdot \dot{y} + C_{mr} \cdot \dot{y} + K_{mr} \cdot y =$$

$$F_{y1} + F_{y2} \quad (8)$$

$$M_e \ddot{y} + y(K_{ml} + K_{mr}) + \dot{y}(C_{ml} + C_{mr}) =$$

$$F_{y1} + F_{y2} \quad (9)$$

From the free body force diagram shown in figure 9, the equilibrium of moment yields the following equations:

$$\sum M = 0 \quad (10)$$

$$J_o \ddot{\theta} + K_{ml}(\theta \cdot Ll) + C_{ml}(\dot{\theta} \cdot Ll) - K_{mr}(\theta \cdot Lr) -$$

$$C_{mr}(\dot{\theta} \cdot Lr) = F_{y1} \cdot a - F_{y2} \cdot b \quad (11)$$

M_e :engine mass [kg], K_{ml} : left side-rubber mount stiffness [N/m], K_{mr} :right side-rubber mount stiffness [N/m], C_{ml} :left side-rubber mount damping [N-s/m], C_{mr} :right side-rubber mount damping [N-s/m], F_{y1} & F_{y2} :excitation force from the 1st & 2nd piston [N].

D. State Variable Model and Block Diagram

From the equation of force and moment equilibrium, the state variable model of the engine dynamic can be developed. Assuming $\dot{y} = v$ and $\dot{\theta} = \omega$, Eq. (9) and (11) can be written as:

$$\dot{v} = \frac{1}{M_e} [-\dot{y}(C_{ml} + C_{mr}) - y(K_{ml} + K_{mr}) + F_{y1} + F_{y2}] \quad (12)$$

$$\dot{\omega} = \frac{1}{J_o} [F_{y1} \cdot a - F_{y2} \cdot b - \theta(K_{ml} \cdot Ll - K_{mr} \cdot Lr) - \dot{\theta}(C_{ml} \cdot Lr - C_{mr} \cdot Lr)] \quad (13)$$

The state variable equation of the system can be written in a general form as:

$$\dot{X} = AX + Bu \quad (14)$$

Where

$$X = [y \quad v \quad \theta \quad \omega]^T$$

$$\dot{X} = [\dot{y} \quad \dot{v} \quad \dot{\theta} \quad \dot{\omega}]^T$$

$$u = \begin{bmatrix} F_{y1} \\ F_{y2} \end{bmatrix}$$

The [A] and [B] matrices can be found in Eq.(15) and (16). Based on the state variable equation of the system, the block diagram is developed and shown in figure 10.

III. RESULT AND DISCUSSION

A. Bouncing of the Engine due to Impulsive Excitation

The bouncing of the engine express the vertical motion of the engine center of mass. Figure 11 to 13 show the bouncing displacement, velocity and acceleration of the engine body due to impulsive excitation. It is shown that the peak amplitude of the displacement due to impulsive excitation is 0.3 μm, the peak amplitude of the velocity

is $8 \mu\text{m/s}$, and the peak amplitude of the acceleration is 1.5 mm/s^2 .

B. Pitching of the Engine due to Impulsive Excitation

The pitching of the engine express the angular motion of the engine body and the center of mass as the center of rotation. Figure 14 to 16 show the pitching displacement, velocity and acceleration of the engine body due to impulsive excitation. It is shown that the peak amplitude of the displacement due to impulsive excitation is $5 \mu\text{-rad}$, the peak amplitude of the velocity is $400 \mu\text{-rad/s}$, and the peak amplitude of the acceleration is 0.2 rad/s^2 .

C. Bouncing of the Engine due to Harmonic Excitation

Figure 17 to 19 show the bouncing displacement, velocity and acceleration of the engine body due to harmonic excitation for the connecting rod length of $L1:115.6 \text{ mm}$. In this numerical work, the connecting rod length was varied for three different value ($L1 = 115.6 \text{ mm}$, $L2 = 125.6 \text{ mm}$, $L3 = 135.6 \text{ mm}$) as well as the engine speed (1000 rpm , 3000 rpm , 5000 rpm). It is shown that the higher the engine speed, the lower the displacement and velocity amplitude. Meanwhile, the acceleration shows the opposite phenomena. This result shows that at high excitation frequency, the amplitude of vibration (displacement and velocity) is lower. However the acceleration is higher. Higher acceleration indicates high shaking force applied to the engine mount structure. As the excitation frequency of the engine depends on the engine speed, the design of engine natural frequency should be made outside its operation frequency.

D. Pitching of the Engine due to Harmonic Excitation

Figure 21 to 22 show the pitching displacement, velocity and acceleration of the engine body due to harmonic excitation for the connecting rod length of $L1:115.6 \text{ mm}$. In this numerical work, the connecting rod length was varied for three different value ($L1 = 115.6 \text{ mm}$, $L2 = 125.6 \text{ mm}$, $L3 = 135.6 \text{ mm}$) as well as the engine speed (1000 rpm , 3000 rpm , 5000 rpm). It is shown that the higher the engine speed, the lower the displacement and velocity amplitude. Meanwhile, the acceleration shows the opposite phenomena. This result shows that at high excitation frequency, the amplitude of vibration (displacement and velocity) is lower. However the acceleration is higher. Higher acceleration indicates high shaking force applied to the engine mount structure. As the excitation frequency of the engine depends on the engine speed, the design of engine natural frequency should be made outside its operation frequency.

Table 2 to 4 show the root mean square of the bouncing and pitching displacement, velocity and acceleration of the engine due to harmonic excitation for various engine speed.

IV. CONCLUSION

A numerical study and analysis of the dynamic behavior of a double cylinder inline 650cc gasoline engine with crank angle 0° for rubber mount is presented in this paper. The numerical study was done by mathematically modeling a double cylinder inline 650cc gasoline engine with crank angle 0° for rubber mount and simulating its dynamic behavior for 3 different connecting rod lengths: 115.6 mm , 125.6 mm , and 135.6 mm . Its mathematical model was developed from the physical model of engine produced by local manufacturer. All parameters used in the simulation are based on the engine specification provided by the manufacturer. In the mathematical model, connecting rod length was varied to investigate its influence to the engine's dynamic behavior. Here, the engine system was modeled as a spring-mass-damper system excited by a periodic force produced by the cylinder working pressure with various excitation frequencies from 1000 rpm to 5000 rpm . The engine's dynamic behavior was indicated by vertical motion (bouncing) and angular motion (pitching) of the engine mass, which is presented in displacement, velocity and acceleration. The results show that connecting rod length does not influence the engine's dynamic behavior. Further, the increase in engine's angular speed/excitation frequency influence significantly the engine's dynamic behavior

ACKNOWLEDGEMENT

This research is part of the main research "Development of a Double Cylinder Inline 650cc Gasoline Engine with Crank Angle 0° ", funded by INSINAS program, Ministry of Research and Technology 2013..

REFERENCES

- [1] W.C.Flower, "Understanding hydraulic mount for improved vehicle noise, vibration and ride qualities", SAE Technical Paper Series 850975, 1985.
- [2] Benjamin B., Jason T. Dreyer, Rajendra Singh, "Experimental study of the hydraulic engine mounts using multiple inertia tracks and orifices: narrow and broad band tuning concepts", Journal of Sound and Vibration, vol.331, p.5209-5223, 2012.
- [3] Song He, Rajendra Singh, "Approximate step response of a nonlinear hydraulic mount using a simplified linear model", Journal of Sound and Vibration, vol.299, p.656-663, 2007.
- [4] J.Christopherson, G.Nakhaie Jazar, "Dynamic behavior comparison of passive hydraulic engine mounts. Part 1: Mathematical analysis", Journal of Sound and Vibration, vol.290, p.1040-1070, 2006.
- [5] J.E.Colgate, C.T.Chang, Y.C.Chiou, W.K.Liu, L.M.Keer, "Modeling of a hydraulic engine mount focusing on response to sinusoidal and composition excitations", Journal of Sound and Vibration, vol.184, p.503-528, 1998.
- [6] H. Adiguna, M. Tiwari, R. Singh, "Transient response of a hydraulic engine mount", Journal of Sound and Vibration, vol.268, p.217-248, 2003.
- [7] A.F.M.S. Amin, M.S. Alam, Y. Okui, "An improved hyperelasticity relation in modeling viscoelasticity response of natural and high damping rubbers in compression: experiments, parameter identification and numerical verification", Journal of Mechanics of Materials, vol.34, p.75-95, 2002.



Figure 1. Physical model of the double cylinder inline 650cc gasoline engine with crank angle 0°

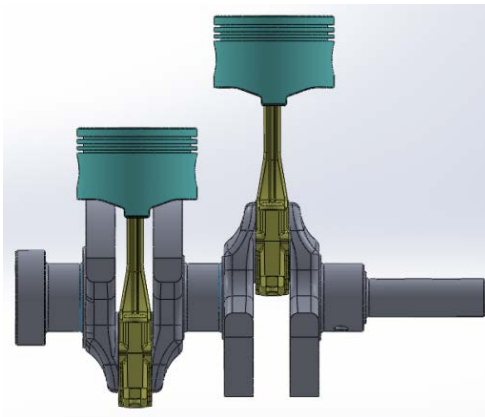


Figure 2. The engine redrawing result

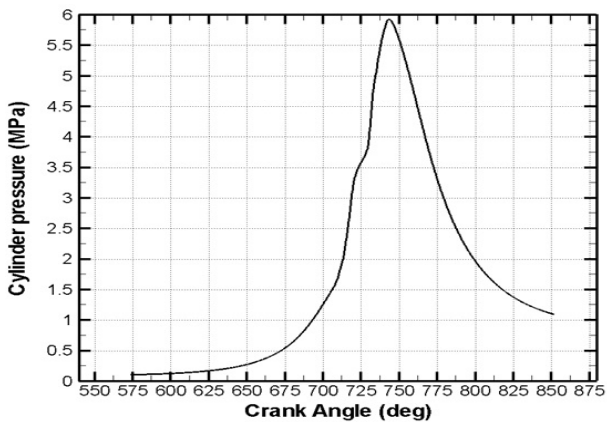


Figure 3. The cycle of cylinder pressure for one cylinder of a double cylinder inline 650cc gasoline engine with crank angle 0°

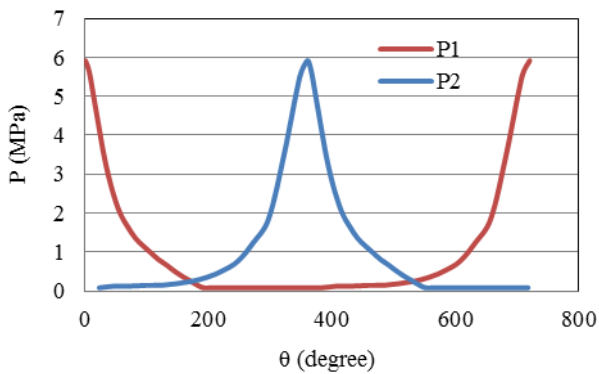


Figure 4. The cycle of cylinder pressure for two cylinder of a double cylinder inline 650cc gasoline engine with crank angle 0°

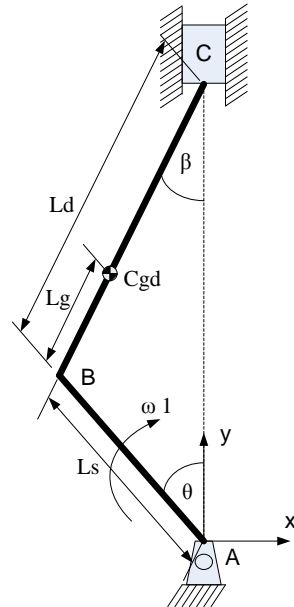


Figure 5. Kinematic diagram of piston, connecting rod and crank shaft

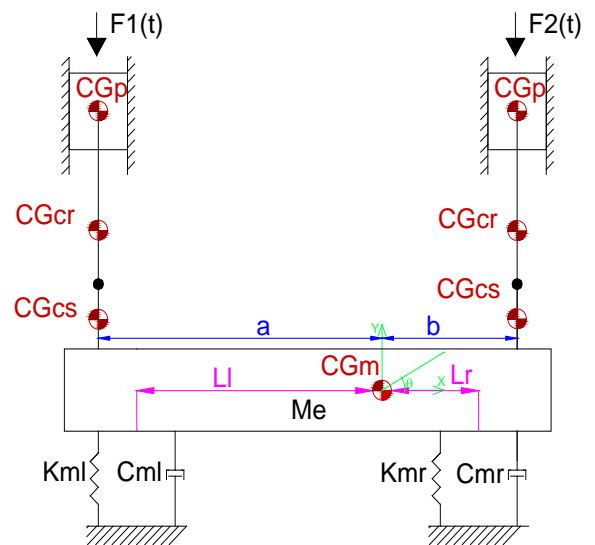


Figure 6. Mathematical model of the engine for front view

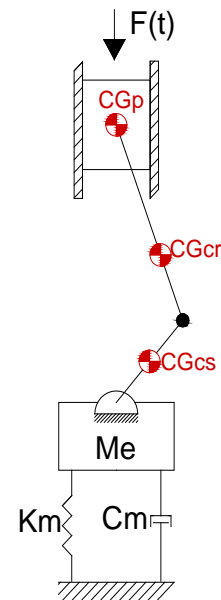


Figure 7. Mathematical model of the engine from side view

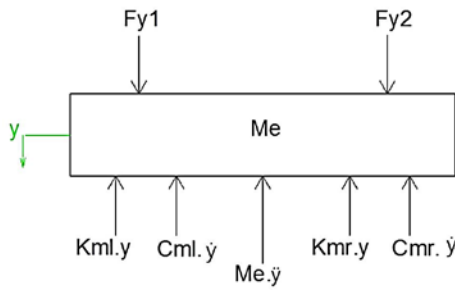


Figure 8. Free body force diagram of the engine

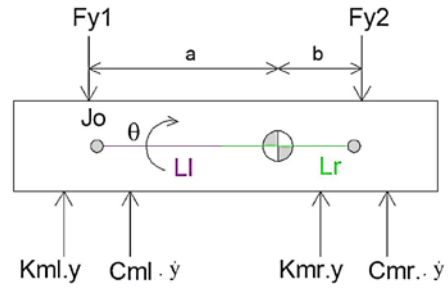


Figure 9. Free body force-moment diagram of the engine

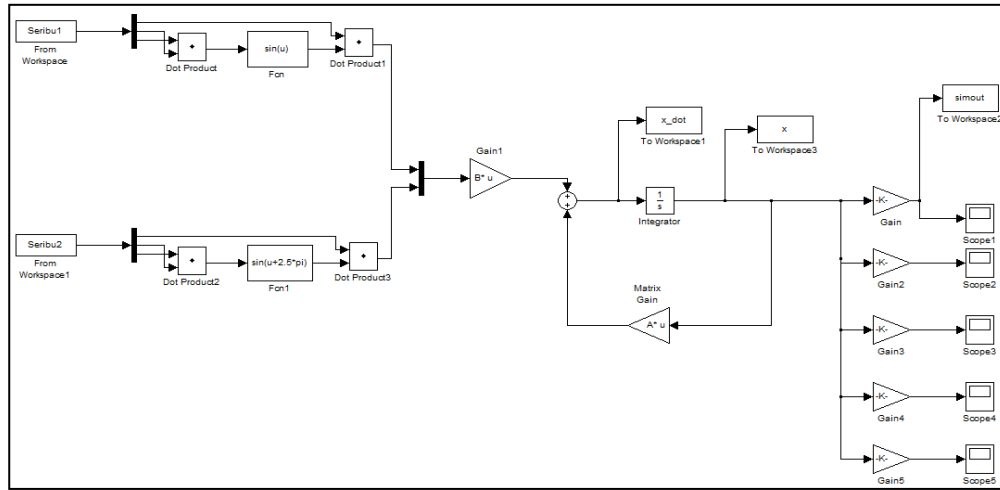


Figure 10. Block diagram of the system

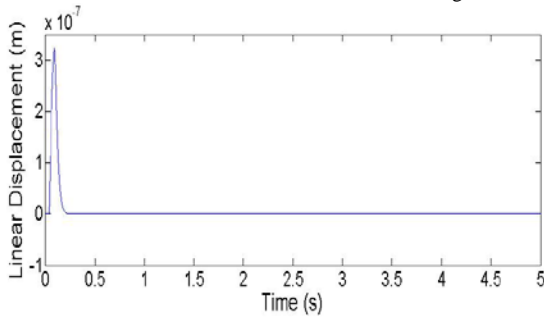


Figure 11. Bouncing displacement of the engine due to impulsive excitation.

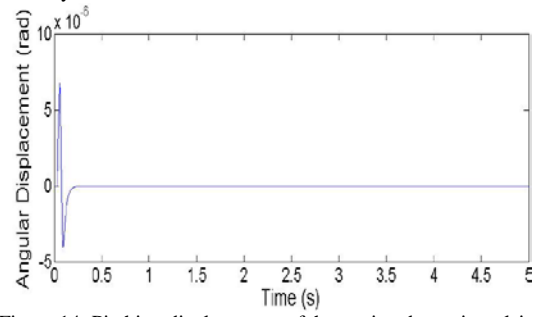


Figure 14. Pitching displacement of the engine due to impulsive excitation

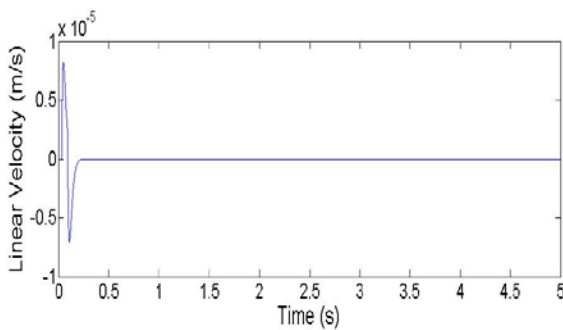


Figure 12. Bouncing velocity of the engine due to impulsive excitation.

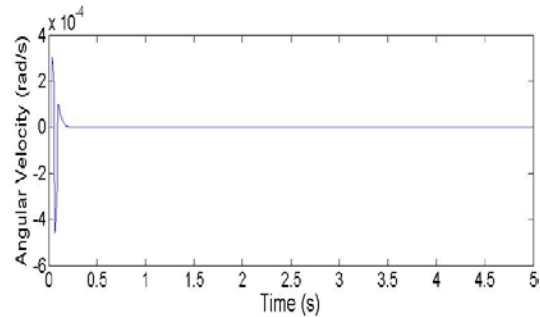


Figure 15. Pitching velocity of the engine due to impulsive excitation

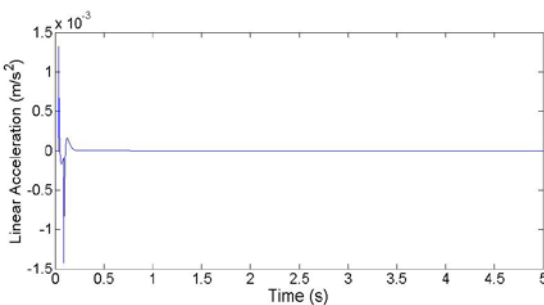


Figure 13. Bouncing acceleration of the engine due to impulsive excitation

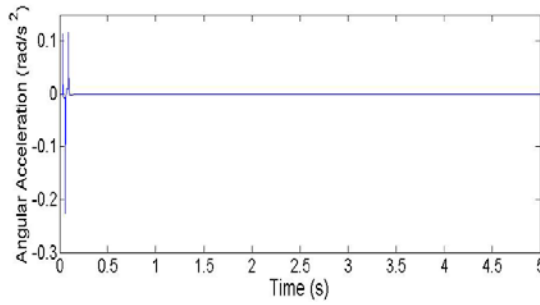


Figure 16. Pitching acceleration of the engine due to impulsive excitation

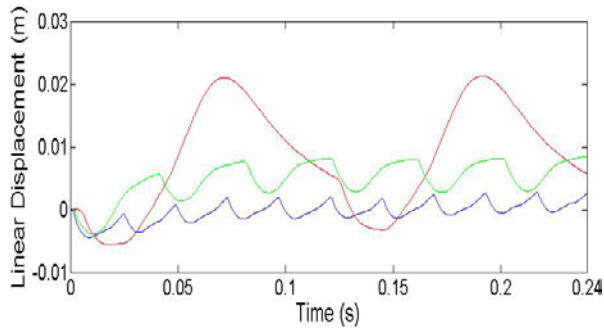


Figure 17. Bouncing displacement of the engine due to harmonic excitation of L1

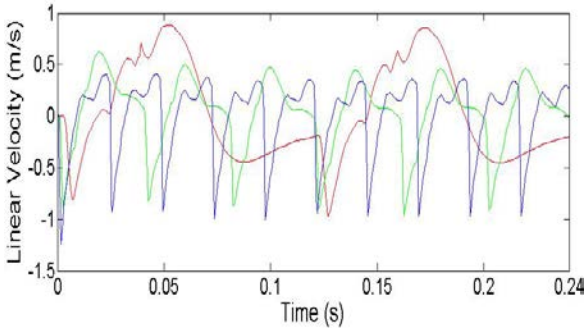


Figure 18. Bouncing velocity of the engine due to harmonic excitation of L1

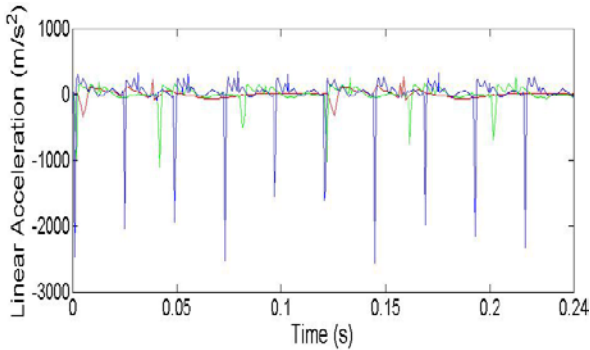


Figure 19. Bouncing acceleration of the engine due to harmonic excitation of L1

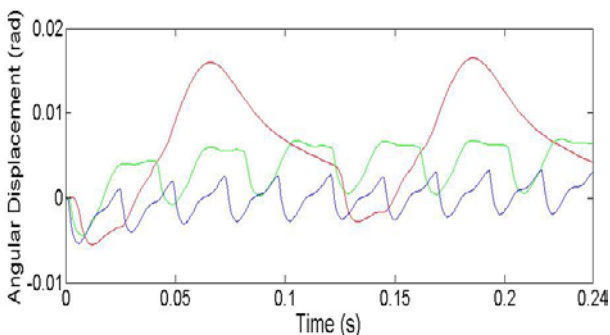


Figure 20. Pitching displacement of the engine due to harmonic excitation of L1

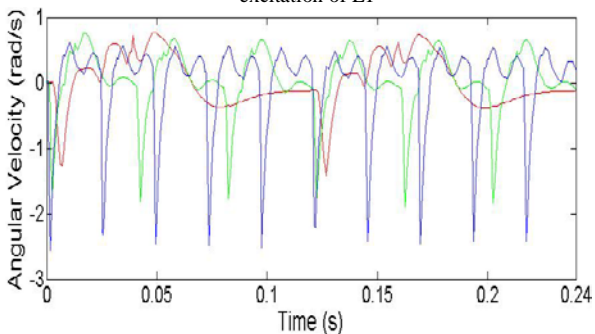


Figure 21. Pitching velocity of the engine due to harmonic excitation of L1

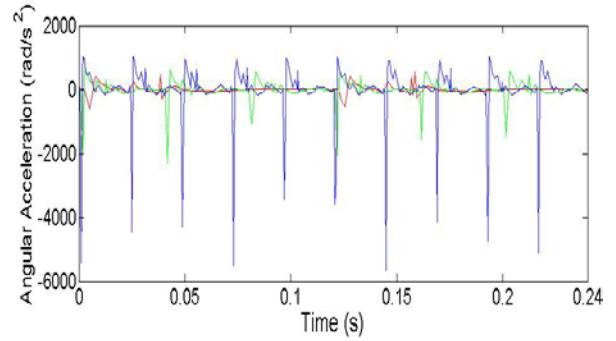


Figure 22. Pitching acceleration of the engine due to harmonic excitation of L1

TABLE 1.
ENGINE PROPERTIES

Engine Properties	Symbol	Value
Angular speed	ω_1	104.7 rps
	ω_2	314 rps
	ω_3	523.3 rps
Crank shaft	L_s	0.04 m
	L_{d1}	0.12 m
	L_{d2}	0.13 m
Connecting rod length	L_{d3}	0.14 m
	L_{g1}	0.024 m
	L_{g2}	0.03 m
Distance from connecting rod center of mass to the pin	L_{g3}	0.03 m
Connecting rod mass	M_d	0.16 kg
Cylinder frontal area	A	4345.3 mm ²
Engine mass	M_e	91 kg
Engine inertia	J_1	0.055 kg.m ²
	J_2	0.058 kg.m ²
	J_3	0.06 kg.m ²
Crank shaft inertia	I_{xx}	0.008 kg.m ²
Distance from the engine center of mass to the support	L_{-1}	0.09 m
Distance from the engine center of mass to the connecting rod	L_r	0.087 m
	a	0.07 m
	b	0.067 m

TABLE 2.
ENGINE PROPERTIES

L1						
rpm	acceleration		velocity		displacement	
	bouncing	pitching	bouncing	pitching	bouncing	pitching
	(m/s ²)	(rad/s ²)	(m/s)	(rad/s)	(m)	(rad)
1000	56,134	89,637	0,471	0,397	0,011	0,009
3000	164,308	306,562	0,335	0,4695	0,005	0,004
5000	416,726	817,064	0,384	0,688	0,001	0,002

TABLE 3.
ENGINE PROPERTIES

L2						
rpm	acceleration		velocity		displacement	
	bouncing	pitching	bouncing	pitching	bouncing	pitching
	(m/s ²)	(rad/s ²)	(m/s)	(rad/s)	(m)	(rad)
1000	64,741	110,836	0,492	0,435	0,011	0,009
3000	175,171	326,331	0,357	0,492	0,005	0,004
5000	419,841	826,201	0,408	0,726	0,002	0,002

TABLE 4.
ENGINE PROPERTIES

L3						
rpm	acceleration		velocity		displacement	
	bouncing	pitching	bouncing	pitching	bouncing	pitching
	(m/s ²)	(rad/s ²)	(m/s)	(rad/s)	(m)	(rad)
1000	61,513	101,639	0,481	0,412	0,012	0,009
3000	174,514	322,159	0,351	0,491	0,005	0,004
5000	433,759	847,453	0,419	0,748	0,002	0,002

$$A = \begin{bmatrix} 0 & 1 & 0 & 0 \\ -\frac{(Kml+Kmr)}{Me} & -\frac{(Cml+Cmr)}{Me} & 0 & 0 \\ 0 & 0 & 0 & 1 \\ 0 & 0 & -\frac{(Kml.Ll-Kmr.Lr)}{Jo} & -\frac{(Cml.Ll-Cmr.Lr)}{Jo} \end{bmatrix} \quad (15)$$

$$B = \begin{bmatrix} 0 & 0 \\ \frac{1}{Me} & \frac{1}{Me} \\ 0 & 0 \\ \frac{1}{Jo} & \frac{1}{Jo} \end{bmatrix} \quad (16)$$